AIAA SciTech Forum
6-10 January 2025, Orlando, FL
AIAA SCITECH 2025 Forum

10.2514/6.2025-0732

Check for updates

On Predicting Magnus Force with Gauss-Constrained PINNs

Abdelrahman Elmaradny *, Mohamed Shorbagy †, Kyle Spink ‡, and Haithem Taha §
Department of Mechanical and Aerospace Engineering, University of California Irvine, Irvine, CA, 92697, USA

The flow around a rotating cylinder has long fascinated fluid mechanicians. Classic potential flow models, while elegant, face limitations in predicting circulation unless augmented by boundary layer modeling and applying the no-slip condition. For rapidly rotating cylinders, separation is suppressed, resulting in an attached boundary layer whose outer flow is a potential-flow with circulation. Adopting this assumption, Glauert matched Prandtl boundary layer over a rapidly rotating cylinder with the outer flow, and managed to determine a series solution for the value of circulation which , in turn, dictates the Magnus lift force. Interestingly, Glauert's results for circulation is independent of viscosity up to the fourth order. This problem has been recently revisited recently, using Gauss' principle of Least Constraint to determine the unknown circulation without any boundary layer calculations. Remarkably, the solution aligns perfectly with Glauert's results derived from the boundary layer solution. The Gauss' principle formulation presents the problem as a one-dimensional optimization problem with the circulation being a free parameter. In this study, we generalize this approach, performing a large-scale optimization to determine the entire flow field (not just the circulation). We utilize a recently developed approach that integrates Physics-Informed Neural Networks (PINNs) with Gauss's principle.

Downloaded by Abdelrahman Elmaradny on August 29, 2025 | http://arc.aiaa.org | DOI: 10.2514/6.2025-0732

I. Introduction

The problem of the normal fluid force acting on a rotating cylinder has a long and rich history, beginning with the early works of pionners such as Robins , Euler and later named after Magnus [1]. This problem has intrigued numerous aerodynamicists, including Rayleigh, Prandtl, and Glauert, and has led to innovative applications in industry, such as Flettner's rotor ship and the modern E-ship 1. Prandtl's hypothesis of a maximum lift coefficient value of 4π [2], based on the coalescence of stagnation points, was later refuted by experiments and simulations that observed higher lift coefficient values [3–5], challenging earlier experimental limits [6–9].

The bifurcation of the flow field that happens as the ratio $\alpha = \frac{\omega R}{U_\infty}$ increases is critical to understanding this problem. Prandtl's observations [7] indicated that when α exceeds 2, the flow separation is suppressed, resembling irrotational flow with circulation. This bifurcation at $\alpha \approx 2$ was confirmed by experiments and simulations [5, 10–13], although some studies reported different critical α values at various Reynolds numbers [14, 15]. For instance, Badr et al. [16] observed vortex shedding suppression at $\alpha = 3$ for certain Reynolds number ranges. The extensive literature includes notable works by Bryant et al. [17], Swanson [18], and others, underscoring the topic's rich and complex nature.

Inspired by the work of Gonzalez and Taha [19–21], which approached the aerodynamics problem through minimization, Gauss' principle was applied to the problem of a rapidly rotating cylinder using the standard model of irrotational flow with unknown circulation outside the boundary layer [22]. This approach involved solving for the circulation by minimizing the deviation between the free motion and the constrained one. Remarkably, this simple one-Dimensional minimization problem, without explicitly considering viscosity, yielded results that matched Glauert's findings, which were derived from complex solutions of boundary layer nonlinear partial differential equations. Additionally, unlike Glauert's solution that is limited to large α values, the analytical solution derived from Gauss' principle is able to predict a bifurcation and a change in physics at $\alpha = \sqrt{6} = 2.45$.

In this work, we extend the parameterization of the flow field by incorporating the capabilities of Physics Informed Neural Networks (PINNs) guided by the Principle of Minimum Pressure Gradient, as applied to fluid mechanics problems [23–25], rather than relying on a single assumed free parameter of circulation. The proposed model yielded excellent results across both regimes, for values of α less than and greater than $\sqrt{6}$. This novel approach, combined with the potential model, shows promise as an efficient solver. When integrated with conformal mapping, it has the potential

*PhD Student, Department of Mechanical and Aerospace Engineering, University of California Irvine, AIAA member
†PhD Candidate, Department of Mechanical and Aerospace Engineering, University of California Irvine, AIAA member
‡Undergraduate Student, Department of Mechanical and Aerospace Engineering, University of California Irvine
§Assosiate Professor, Department of Mechanical and Aerospace Engineering, University of California Irvine, and AIAA Associate Fellow

Copyright © 2025 by the American Institute of Aeronautics and Astronautics, Inc. All rights reserved.

to significantly advance the study and resolution of complex aerodynamics problems at the limit of infinity Reynold's number.

II. Theoretical Background

In his work, Gauss [26] introduced one of the foundational principles of classical mechanics, known as the "Principle of Least Constraint". This principle states that the motion of a system of 'N' material points occurs in a manner that minimally deviates from free motion, with the measure of constraint being the sum of the products of mass and the square of the deviation from free motion. Gauss distinguished between two types of acceleration: the free acceleration ($a_{\text{free}} = \frac{F}{m}$)), which is the acceleration a body would have without constraints, and the true acceleration, which occurs in the presence of constraints. The difference between these accelerations represents the constraint force, and according to Gauss' principle, the sum of these constraint forces must be minimized at every moment.

Gauss' principle implies that a constrained body will follow the path that minimizes deviation from free motion, expressed mathematically as:

$$Z = \sum_{i=1}^{N} m_i \left(a_i - \frac{F_i}{m_i} \right)^2 \tag{1}$$

This minimization is akin to the least squares method, as Gauss noted the similarity by comparing it to how mathematicians reconcile results through least squares. To illustrate this principle, consider the motion of a pendulum, where the pendulum's mass is constrained to move along a circular-shaped trajectory. The Gaussian constraint Z is calculated based on the pendulum's tangential and normal accelerations, leading to the familiar equation of motion derived through Classical Newtonian laws. Gauss' principle operates instantaneously, *optimizing* acceleration at each moment, in contrast to the integral approach of the principle of least action, which optimizes the entire trajectory over time. In the absence of applied forces $F = 0$, Gauss' principle simplifies to Hertz' principle of least curvature [27], further emphasizing its foundational role in analytical mechanics.

When applied to fluid mechanics problems, Gauss' principle is an efficient method for transforming problems into minimization problems rather than formulating them as partial differential equations. Although Gauss' principle has been integrated into analytical mechanics, it was not widely recognized for solving problems that other techniques couldn't address [28]. Variational techniques in fluid mechanics have traditionally been limited by the dissipative nature of fluids, but recently, applying Gauss' principle to fluid mechanics problems has shown success and has been termed the Principle of Minimum Pressure Gradient (PMPG) [29–31].

The PMPG states that the pressure force is a constraint force whose sole role is maintaing the constraint of the continuity equation. According to Gauss' principle, this constraint force is minimized at each moment, ensuring nature does not exert more force than required. The strength of this principle lies in its ability to handle arbitrary forces, not just conservative ones as in the principle of least action. Mathematically, PMPG involves minimizing the cost $\mathcal{A}$, which is the integral of the pressure gradient over the computational domain:

$$\mathcal{A} = \frac{1}{2}\rho \int_{\Omega} \left(\frac{\partial \mathbf{u}}{\partial t} + (\mathbf{u} \cdot \nabla)\mathbf{u} - \frac{1}{\rho}\nabla \cdot \tau \right)^2 d\mathbf{x}.$$

III. PMPG guided PINNs

Recent advancements in neural networks have sparked growing interest in tackling fluid mechanics problems through "data-free" Physics-Constrained Neural Networks. This innovative computational framework employs neural networks guided by the fundamental physical governing equations, eliminating the reliance on external datasets.

Unlike traditional methods that depend on solving partial differential equations or leveraging data-driven optimization, this variant of Physics-Informed Neural Networks (PINNs) emphasizes the direct minimization of certain physical quantities. Earlier studies by Nguyen-Thanh et al. [32] and Goswami [33] illustrated the effectiveness of similar approaches in structural mechanics and brittle fracture problems, respectively.

Recent progress in fluid mechanics has shown the efficacy of employing the Principle of Minimum Pressure Gradient (PMPG) within the PINNs platform. This framework has been successfully applied to inviscid flow over a cylinder [23, 25] and lid-driven cavity flows [24], demonstrating its potential for solving complex flow scenarios with reduced computational cost and enhanced physical consistency.

Downloaded by Abdelrahman Elmaradny on August 29, 2025 | http://arc.aiaa.org | DOI: 10.2514/6.2025-0732

A PINN model can be mathematically expressed as:

$$\mathbf{y}(\mathbf{x}, t; \theta) = F_{NN}(\mathbf{x}, t; \theta) \tag{2}$$

where $\mathbf{y}$ denotes the model's output, $\mathbf{x}$ represents the input, t signifies time, and θ encompasses the parameters of the neural network F_{NN}. These parameters are determined through the network's training process, aimed at minimizing the total loss function $\mathcal{L}$, defined as:

$$\mathcal{L} = \mathcal{L}_{data} + \lambda \mathcal{L}_{physics}, \tag{3}$$

where $\mathcal{L}$ comprises a data loss term $\mathcal{L}_{data}$ and a physics-informed loss term $\mathcal{L}_{physics}$, with weighting coefficient λ controlling the percentage of physical input to the PINNs model. In the case of the PMPG-PINN approach, the minimization quantity is specified as the pressure gradient, leveraging the latest findings in variational fluid mechanics [31].

Integrating the Principle of Minimum Pressure Gradient (PMPG) with Physics-Informed Neural Networks (PINNs) marks a significant advancement. This hybrid approach, PMPG-PINNs, combines the strengths of both methodologies to address complex fluid dynamics challenges more effectively. In PMPG-PINNs, the principle of minimum pressure gradient is embedded in the neural network's learning process through a physics-informed loss function and eliminating the data loss function. This ensures adherence to physical laws while directing the neural network to minimize the pressure gradient in fluid flow. The network's architecture and training process remain similar to standard PINNs, but the cost function is augmented to include a term representing the PMPG:

$$\mathcal{L}_{PMPG} = \sum \left| \frac{\partial \mathbf{u}}{\partial t} + (\mathbf{u} \cdot \nabla)\mathbf{u} - \nu \nabla^2 \mathbf{u} \right|^2 \tag{4}$$

By reformulating the Navier-Stokes equations in terms of the velocity field and its derivatives, this approach avoids the explicit need for the calculation of the pressure field. The resultant optimization problem for a steady problem minimizes the integral of pressure gradient squared over the domain, constrained by mass and momentum conservation and boundary conditions:

$$\begin{aligned} \min_{\mathbf{u}(\mathbf{x};\theta)} \quad & \mathcal{A} = \frac{1}{2} \int_{\Omega} \rho \Big((\mathbf{u} \cdot \nabla)\mathbf{u} - \nu \nabla^2 \mathbf{u} \Big)^2 d\mathbf{x} \\ \text{s.t.} \quad & \nabla \times \Big((\mathbf{u} \cdot \nabla)\mathbf{u} - \nu \nabla^2 \mathbf{u} \Big) = 0, \\ & \nabla \cdot \mathbf{u} = 0, \\ & \mathbf{u} \cdot \mathbf{n} = 0, \quad \text{on } \delta\Omega, \\ & (\mathbf{u} - \mathbf{u}_{wall}) \cdot \mathbf{t} = 0, \quad \text{on } \delta\Omega \end{aligned} \tag{5}$$

where $\mathbf{n}$, $\mathbf{t}$ are normal and tangential vectors to the boundary $\delta\Omega$. The first constraint of $\nabla \times ((\mathbf{u} \cdot \nabla)\mathbf{u} - \nu \nabla^2 \mathbf{u}) = 0$ employs the vorticity transport equation to enforce the conservation of momentum without the need for a coupled velocity-pressure equation. The second constraint of $\nabla \cdot \mathbf{u} = 0$ ensures the conservation of mass. While the third and fourth constraints are for the no-penetration and no-slip boundary conditions respectively.

IV. Problem formulation

The problem addressed in this research is modeled as a steady potential flow over a rotating cylinder. The governing equations are simplified to omit all terms in the cost function but for the non-linear convective acceleration. The free motion, that the flow would have followed if there were no constraints, can be derived from the potential motion due to a point vortex centered at the cylinder origin of strength Γ_ω. This point vortex induces a purely tangential velocity $u_\theta(r, \theta) = \frac{\Gamma_\omega}{2\pi r}$ which corresponds to ωR on the circumference. The vortex strength Γ_ω thus is equivalent to $2\pi R^2 \omega$ and the corresponding free acceleration given by:

$$a_{\text{free}} = -\frac{u_\theta^2}{r} \hat{e_r}, \tag{6}$$

in the radial direction.

The conservation of momentum can be satisfied by utilizing the vorticity transport equation, where the curl of the momentum equation is taken to satisfy the equilibrium constraintSince, the pressure gradient and the forcing term a_{free}

Downloaded by Abdelrahman Elmaradny on August 29, 2025 | http://arc.aiaa.org | DOI: 10.2514/6.2025-0732

Downloaded by Abdelrahman Elmaradny on August 29, 2025 | http://arc.aiaa.org | DOI: 10.2514/6.2025-0732

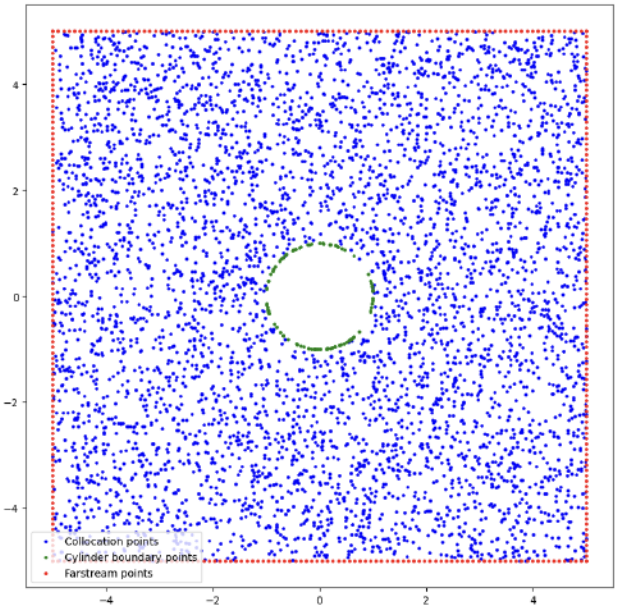

Fig. 1 Domain points used for training in blue, Points on the cylinder in green and the points for Far-Field in red .

both come from a gradient of a potential, and with the inviscid assumption, the equilibrium constraint used reduces to equating the curl of the convective acceleration $\nabla \times \Big((\mathbf{u}\cdot\nabla)\mathbf{u}\Big)$ to zero.

This reduces the problem to a constrained minimization problem implementing the same approach investigated by Atallah et al. [23], Elmaradny et al. [25] to formulate the problem using the PMPG-PINN as follows:

$$\begin{aligned} \min_{\mathbf{u}(\mathbf{x};\boldsymbol{\theta})} \quad & \frac{1}{2}\int_{\Omega} \rho\Big((\mathbf{u}\cdot\nabla)\mathbf{u} + \frac{\Gamma_\omega^2}{4\pi^2 r^3}\hat{e_r}\Big)^2 d\mathbf{x} \\ \text{s.t.} \quad & \nabla \times \Big((\mathbf{u}\cdot\nabla)\mathbf{u}\Big) = 0, \\ & \nabla\cdot\mathbf{u} = 0, \\ & \mathbf{u}\cdot\mathbf{n} = 0, \quad \text{on } \delta\Omega \end{aligned} \tag{7}$$

Translating this to loss functions using the penalty method to satisfy the Boundary condition, FarField condition and the Equilibrium gives us the following:

$$\mathcal{L}_{Total}(\mathbf{x};\theta) = \lambda_1\mathcal{L}_{PMPG} + \lambda_2\mathcal{L}_{BC} + \lambda_3\mathcal{L}_{FFC} + \lambda_4\mathcal{L}_{Eqm}, \tag{8}$$

where $\mathcal{L}_{PMPG}$ is the main loss function in this problem given as:

$$\mathcal{L}_{PMPG} = \sum \Big|(\mathbf{u}\cdot\nabla)\mathbf{u} + \frac{\Gamma_\omega^2}{4\pi^2 r^3}\hat{e_r}\Big|^2, \tag{9}$$

$\mathcal{L}_{BC}$ the no-penetration boundary condition, $\mathcal{L}_{FFC}$ the Far-Field condition and $\mathcal{L}_{Eqm}$ the equilibrium constraint of the conservation of momentum weighted by their respective λ_n.

When the problem is solved analytically [22] as a one-dimensional minimization problem with a single free parameter Γ, minimizing the cost $\mathcal{A}$ yielded three roots:

$$\Gamma^* = \pm 4\pi R\sqrt{\frac{\omega^2 R^2}{4} - \frac{3U_\infty^2}{2}},\ 0 \tag{10}$$

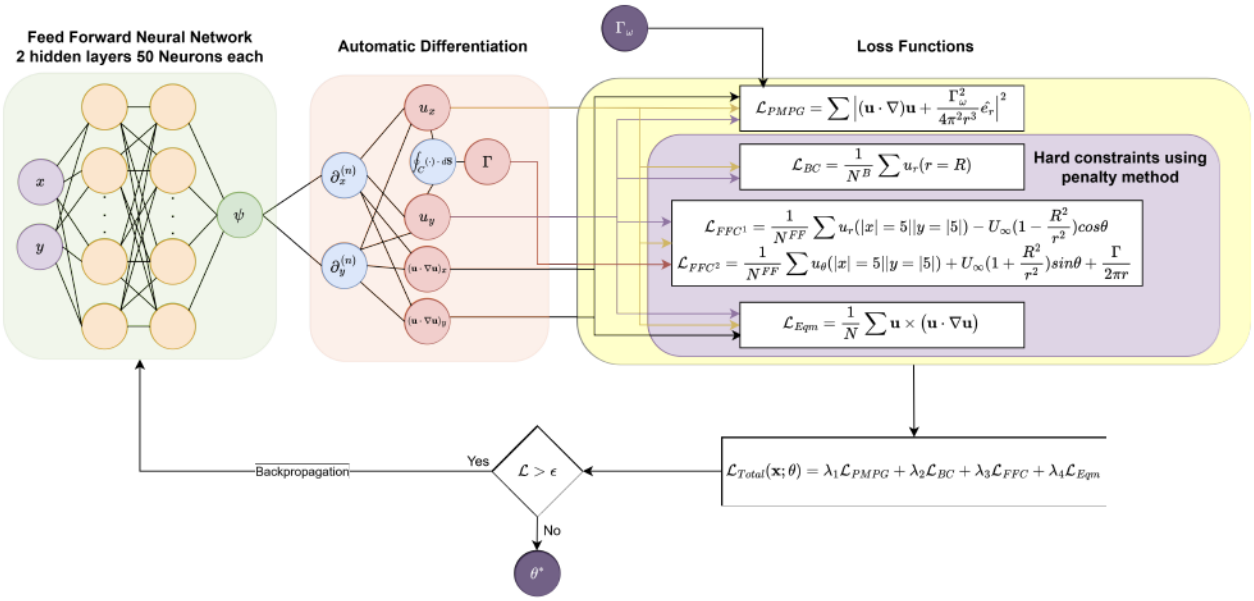

Fig. 2 Schematic of the PMPG-PINN formulation applied to the problem of flow over rotating cylinder as well as the Neural Network structure.

The ± values of Γ^* occur because the formulation is agnostic to the direction of rotation; the circulation direction is predetermined by the cylinder's rotation direction. Equation (10) indicates a critical angular rotation value $\omega_{cr} = \sqrt{6}\frac{U_\infty}{R}$. Below this critical value, the first two roots are imaginary, making the zero circulation the only physical root and the global minimizer the flow chooses. Beyond ω_{cr}, all roots become real, with the first two being global minimizers and the zero root being a maximizer hence accounting for the bifurcation of the physics of the problem.

V. Implementation

To address the 2D nature of the problem, the streamfunction ψ is used as the output of the Neural Network to inherently satisfy the conservation of mass. By differentiating ψ, we obtain the velocity components in the x and y directions, u_x and u_y, respectively:

$$u_x = \frac{\partial \psi}{\partial y}, \qquad u_y = -\frac{\partial \psi}{\partial x}. \tag{11}$$

The selected problem domain features a 2D cylinder with a unit radius, surrounded by 5000 randomly sampled points within a square of area ten times the cylinder's radius. Along the cylinder's circumference, 200 randomly distributed boundary points enforce the No-Penetration condition using the penalty method [34], ensuring radial velocity is zero at these points. Additionally, 100 points are placed on each boundary edge to satisfy the FarField condition. The grid points of training are shown in Figure 1.

The FarField boundary condition acts as the driver for the flow to become a superposition between a flow over cylinder and a rotating cylinder, it is not accurate to assume in the finite domain we have that the flow at the boundary points is unity in the x-direction as in the case of the flow over cylinder without circulation. To satisfy this in the model a feedback constraint on the FarField boundary points is imposed, where the velocity at the FarField points takes the form of an irrotational flow over a rotating cylinder, with the circulation Γ being calculated from the points on the cylinder boundary:

$$\begin{aligned} u_r(|x| = 5||y = |5|) &= U_\infty(1 - \tfrac{R^2}{r^2})cos\theta \\ u_\theta(|x| = 5||y = |5|) &= -U_\infty(1 + \tfrac{R^2}{r^2})sin\theta - \tfrac{\Gamma}{2\pi r}. \end{aligned} \tag{12}$$

This ensures that at each iteration of training, the values of velocities on the boundaries are coupled to the circulation on

Downloaded by Abdelrahman Elmaradny on August 29, 2025 | http://arc.aiaa.org | DOI: 10.2514/6.2025-0732

Downloaded by Abdelrahman Elmaradny on August 29, 2025 | http://arc.aiaa.org | DOI: 10.2514/6.2025-0732

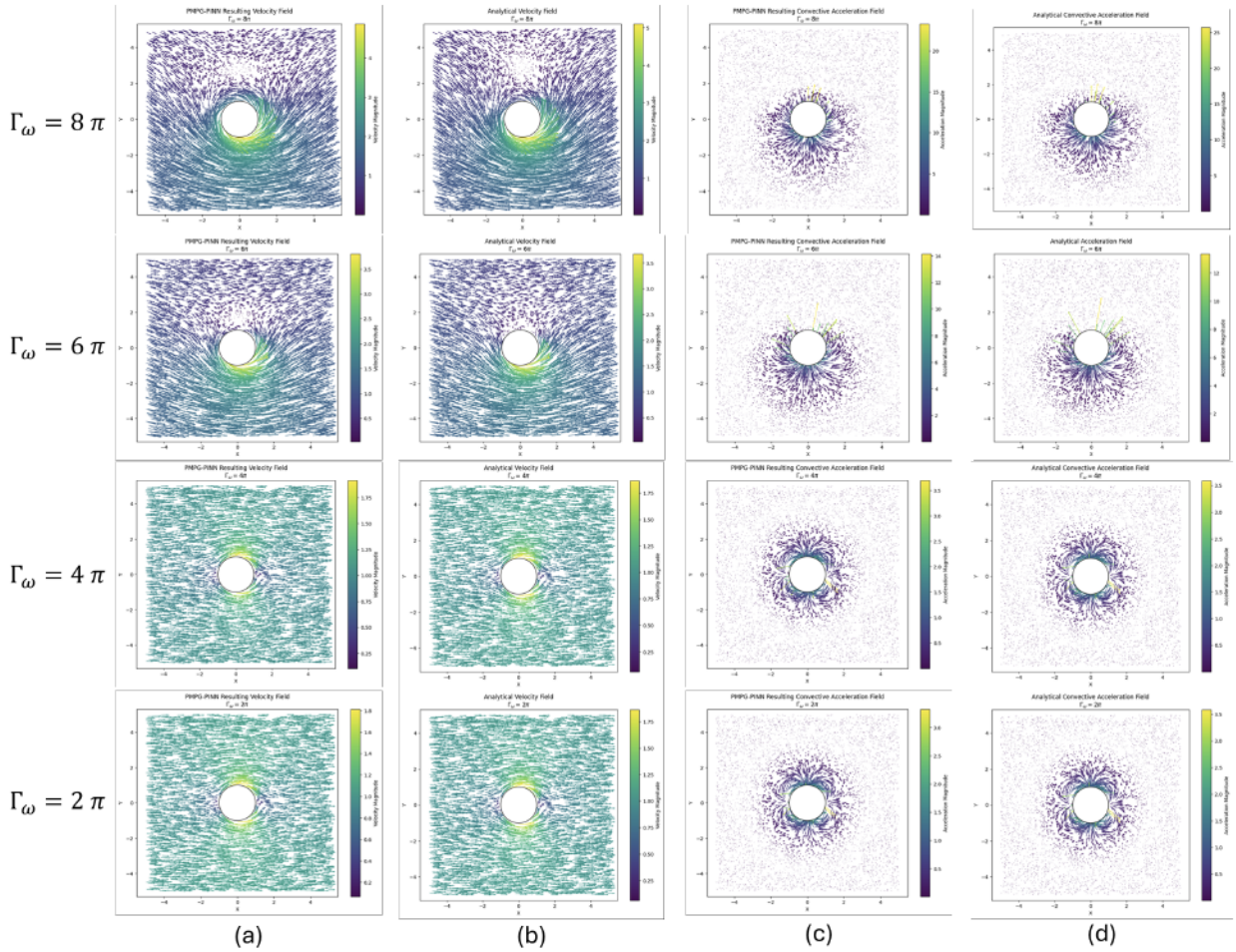

Fig. 3 Velocity and convective acceleration fields for the four cases at $\Gamma_\omega = 2\pi, 4\pi, 6\pi$ and 8π (a) PMPG-PINN generated velocity fields, (b) Analytical velocity fields, (c) PMPG-PINN generated convecevtive acceleration fields and (d) Analytical convective acceleration fields.

the cylinder surface.

The Neural Network employed is a Feed-Forward Fully-Connected Neural Network with two hidden layers, each containing 50 neurons. The input layer has two neurons for the spatial coordinates x and y, and the output layer has a single neuron for the streamfunction ψ. The activation function used is the hyperbolic tangent (*Tanh*). Training is performed using the *Adam* optimization algorithm, a stochastic optimization method commonly used for deep neural networks [35]. A comprehensive schematic and structure of the PMPG-PINN model for the rotating cylinder problem is shown in Figure 2,

VI. Results

It has been previously shown by Shorbagy et al. [22] that there is a critical value for Γ_ω at 4.89π, below which the flow field will not sense the rotation. The simulations were carried for four different values for Γ_ω: $2\pi, 4\pi, 6\pi$ and 8π. Qualitative comparison between the generated velocity fields and the analytical one (illustrated in Figure 3), clearly shows that the velocity fields of 2π and 4π cases (below the critical Γ_ω don't sense the rotation, and converge to the well-known flow over cylinder flow without circulation. As the Γ_ω increases to values more than the critical one, namely at 6π and 8π, the solver retrieves the results obtained from analytical solutions.

The RMS Error of the obtained velocity fields shows a good match between the PMPG-PINN generated models and the analytical solutions. The RMS Error didn't exceed 0.0853 and it increased with the increase in Γ_ω as shown in

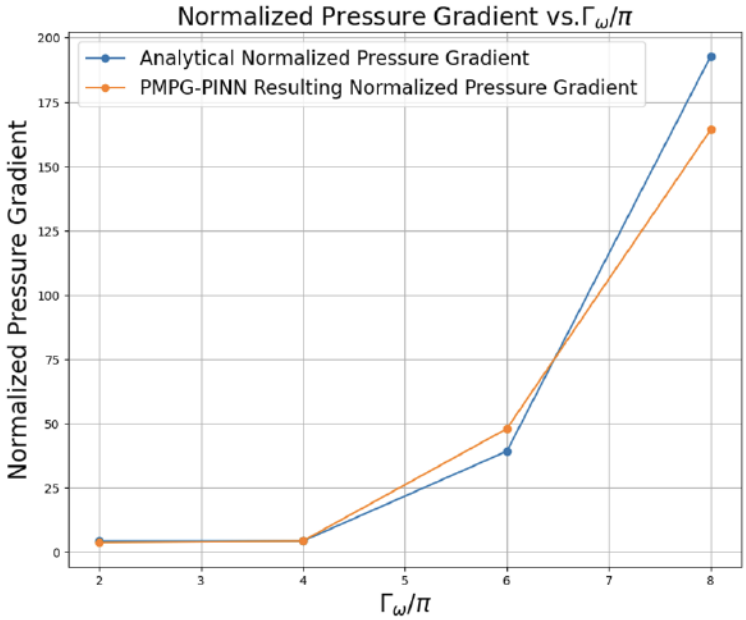

Fig. 4 Normalized pressure gradient obtained from PMPG-PINN solver and that of the analytical solution on the same grid for different Γ_ω values.

Table 1.

Another physical metric relied on to quantitatively evaluate the results is the normalized pressure gradient. Figure 4 demonstrates the proximity between the solver's normalized pressure gradient and the expected ones from the analytical solution on the same grid. Table 1 demonstrates the RMS error of the velocity fields as well as Normalized Pressure gradient compared to the analytical ones.

Table 1 RMS Error magnitudes for velocity fields and normalized pressure gradients

Γ_ω	RMS Error Value	Normalized Analytical Pressure Gradient	Normalized PMPG-PINNs Pressure Gradient
2π	0.008	4.3684	3.8608
4π	0.0137	4.3684	4.4091
6π	0.0725	39.2821	48.0129
8π	0.0853	192.7675	164.2493

The main metric that is decisive of the flow rotation is the circulation Γ. It is already discussed from Eq. 10, the relationship between Γ^* and Γ_ω. Assuming unity values for the cylinder radius R and the free-stream velocity U_∞, the equation is reduced to :

$$\Gamma^* = \begin{cases} \Gamma_\omega \sqrt{1 - \frac{6(4\pi)^2}{\Gamma_\omega^2}} & \Gamma_\omega > 4.89\pi \\ 0 & \Gamma_\omega < 4.89\pi \end{cases} \tag{13}$$

applicable for values of Γ_ω larger than the critical value of 4.89π. Any Γ_ω below this value gives a zero circulation to the fluid. Figure 5 overlays the circulation of the simulated flows over the analytical ones of Eq. 13. For Γ_ω values below the critical value, the circulation of the obtained velocity fields is almost zero, while it has values matching those of the analytical solution for Γ_ω larger than the critical value.

Downloaded by Abdelrahman Elmaradny on August 29, 2025 | http://arc.aiaa.org | DOI: 10.2514/6.2025-0732

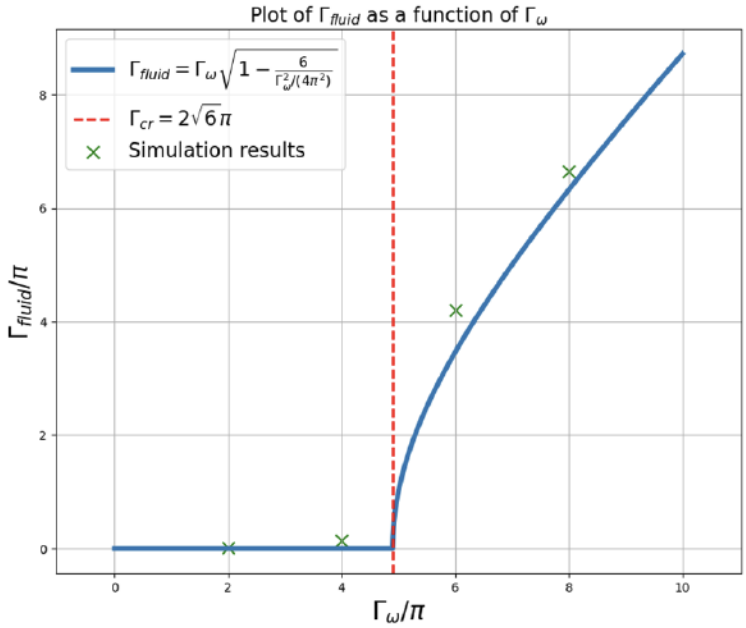

Fig. 5 Comparison between the circulation obtained from the solver Γ vs the imposed circulation Γ_ω with cylinder radius $R = 1$, $U_\infty = 1$.
The blue curve is the analytical solution as per Gauss' principle in Eq 13 and the green x marks are the PMPG-PINN generated simulations at different Γ_ω values.

VII. Conclusions

In this work, we have integrated Physics-Informed Neural Networks (PINNs) with Gauss's principle of least constraint to tackle the problem of the flow around a rotating cylinder. This novel approach allowed large-scale parametrization of the flow field using the weights and biases of the Neural Network, that is, the fluid mechanics problem is converted into a large-scale minimization problem. The optimizer predicted zero circulation at lower rotational speeds (e.g., $\Gamma_\omega = 2\pi, 4\pi$), consistent with theoretical expectations derived from Gauss's Principle, while resulting in non-zero circulation as rotational speed increased beyond $\omega_{cr} = \sqrt{6}$ corresponding to critical $\Gamma_\omega = 4.89\pi$.

Our findings demonstrate the efficacy of using PINNs coupled with variational principles for fluid dynamics problems. This approach not only offers a computationally efficient alternative to traditional methods but also opens avenues for revisiting various aerodynamic challenges using conformal mapping and inviscid flow assumptions.

The combination of solving this problem and conformal mapping represents a powerful approach to address a wide range of aerodynamic problems efficiently and accurately. By leveraging PINNs, which are adept at learning complex physical relationships from data, and guiding them with variational principles like Gauss's Principle, we can effectively model fluid dynamics problems without the computational burden of solving complex partial differential equations explicitly.

Acknowledgments

The authors would like to acknowledge the support from the National Science Foundation grant number CBET-2332556 and the Air Force Office of Scientific Research under award number FA9550-22-1-0386, monitored by Dr. Gregg Abate.

References

[1] Tokaty, G. A., *A history and philosophy of fluid mechanics*, Courier Corporation, 1994.

[2] Prandtl, L., "Magnuseffekt und Windkraftschiff," *The science of nature*, Vol. 13, No. 6, 1925, pp. 93–108. https://doi.org/doi.org/10.1007/BF01585456.

Downloaded by Abdelrahman Elmaradny on August 29, 2025 | http://arc.aiaa.org | DOI: 10.2514/6.2025-0732

[3] Tokumaru, P., and Dimotakis, P., "The lift of a cylinder executing rotary motions in a uniform flow," *Journal of fluid mechanics*, Vol. 255, 1993, pp. 1–10. https://doi.org/10.1017/S0022112093002368.

[4] Mittal, S., "Flow past rotating cylinders: effect of eccentricity," *J. Appl. Mech.*, Vol. 68, No. 4, 2001, pp. 543–552. https://doi.org/10.1115/1.1380679.

[5] Mittal, S., and Kumar, B., "Flow past a rotating cylinder," *Journal of fluid mechanics*, Vol. 476, 2003, pp. 303–334. https://doi.org/10.1017/S0022112002002938.

[6] Reid, E., "Tests of rotating cylinders. NACA Tech," Tech. rep., Note 209, 1924. URL https://ntrs.nasa.gov/api/citations/19930080991/downloads/19930080991.pdf.

[7] Prandtl, L., and Tietjens, O., "Hydro-und Aeromechanik. Bd," , 1931. https://doi.org/10.1007/978-3-7091-5042-9_1.

[8] Thom, A., *The pressures round a cylinder rotating in an air current*, HM Stationery Office, 1927.

[9] Thom, A., "Experiments on the flow past a rotating cylinder," Tech. rep., HM Stationery Office, 1931. URL https://reports.aerade.cranfield.ac.uk/handle/1826.2/1419.

[10] Coutanceau, M., and Menard, C., "Influence of rotation on the near-wake development behind an impulsively started circular cylinder," *Journal of Fluid Mechanics*, Vol. 158, 1985, pp. 399–446. https://doi.org/10.1017/S0022112085002713.

[11] Badr, H., and Dennis, S., "Time-dependent viscous flow past an impulsively started rotating and translating circular cylinder," *Journal of Fluid Mechanics*, Vol. 158, 1985, pp. 447–488. https://doi.org/10.1017/S0022112085002725.

[12] Diaz, F., Gavaldà, J., Kawall, J., Keffer, J., and Giralt, F., "Vortex shedding from a spinning cylinder," *The Physics of fluids*, Vol. 26, No. 12, 1983, pp. 3454–3460. https://doi.org/10.1063/1.864127.

[13] Degani, A., Walker, J., and Smith, F., "Unsteady separation past moving surfaces," *Journal of Fluid Mechanics*, Vol. 375, 1998, pp. 1–38. https://doi.org/10.1017/S0022112098001839.

[14] Kang, S., Choi, H., and Lee, S., "Laminar flow past a rotating circular cylinder," *Physics of Fluids*, Vol. 11, No. 11, 1999, pp. 3312–3321. https://doi.org/10.1063/1.870190.

[15] Barnes, F., "Vortex shedding in the wake of a rotating circular cylinder at low Reynolds numbers," *Journal of Physics D: Applied Physics*, Vol. 33, No. 23, 2000, p. L141. https://doi.org/10.1088/0022-3727/33/23/101.

[16] Badr, H., Coutanceau, M., Dennis, S., and Menard, C., "Unsteady flow past a rotating circular cylinder at Reynolds numbers 103 and 104," *Journal of Fluid Mechanics*, Vol. 220, 1990, pp. 459–484. https://doi.org/10.1017/S0022112090003342.

[17] Bryant, L., Williams, D., and Taylor, G., "An Investigation of the Flow of Air around an Aerofoil of Infinite Span," *Philosophical Transactions of the Royal Society of London. Series A, Containing Papers of a Mathematical or Physical Character*, Vol. 225, 1926, pp. 199–245. https://doi.org/10.1098/rsta.1926.0005.

[18] Swanson, W., "The Magnus effect: A summary of investigations to date," 1961. https://doi.org/10.1115/1.3659004.

[19] Gonzalez, C., and Taha, H. E., "A Variational Theory of Lift," *Journal of Fluid Mechanics*, Vol. 941, 2022. https://doi.org/doi.org/10.1017/jfm.2022.348.

[20] Taha, H. E., and Gonzalez, C., "Refining Kutta's Flow over a Flat Plate: Necessary Conditions for Lift," *AIAA Journal*, Vol. 61, No. 5, 2023, pp. 2060–2068.

[21] Taha, H. E., and Gonzalez, C., "The flow over a flat plate: Did kutta get it right?" *AIAA SCITECH 2022 Forum*, 2022, p. 1665.

[22] Shorbagy, M., and Taha, H., "Magnus Force Estimation Using Gauss's Principle of Least Constraint," *AIAA Journal*, 2024, pp. 1–8.

[23] Atallah, A., Elmaradny, A., and Taha, H. E., "A Novel Approach for Data-Free, Physics-Informed Neural Networks in Fluid Mechanics Using the Principle of Minimum Pressure Gradient," *AIAA SCITECH 2024 Forum*, 2024, p. 2742.

[24] Alhussein, H., and Daqaq, M., "The principle of minimum pressure gradient: An alternative basis for physics-informed learning of incompressible fluid mechanics," *AIP Advances*, Vol. 14, No. 4, 2024, p. 045112. https://doi.org/10.1063/5.0197860, URL https://doi.org/10.1063/5.0197860.

[25] Elmaradny, A., Atallah, A., and Taha, H., "Minimizing Nature's Cost: Exploring Data-Free Physics-Informed Neural Network Solvers for Fluid Mechanics Applications," , 2024. URL https://arxiv.org/abs/2411.15410.

Downloaded by Abdelrahman Elmaradny on August 29, 2025 | http://arc.aiaa.org | DOI: 10.2514/6.2025-0732

[26] Gauss, C. F., "Über ein neues allgemeines Grundgesetz der Mechanik." 1829. https://doi.org/10.1515/crll.1829.4.232.

[27] Papastavridis, J., *Analytical mechanics: a comprehensive treatise on the dynamics of constrained systems – Reprint edition.*, Word Scientific Publishing Company, 2014.

[28] Papastavridis, J., *Analytical Mechanics: A Comprehensive Treatise on the Dynamics of Constrained Systems*, World Scientific Publishing Company, 2014. Reprint edition.

[29] Taha, H. E., and Gonzalez, C., "What does nature minimize in every incompressible flow?" *arXiv preprint arXiv:2112.12261*, 2021.

[30] Taha, H. E., and Gonzalez, C., "A Variational Principle for Navier-Stokes Equations," *AIAA SCITECH 2023 Forum*, 2023, p. 1432.

[31] Taha, H., Gonzalez, C., and Shorbagy, M., "A minimization principle for incompressible fluid mechanics," *Physics of Fluids*, Vol. 35, No. 12, 2023.

[32] Nguyen-Thanh, V. M., Zhuang, X., and Rabczuk, T., "A deep energy method for finite deformation hyperelasticity," *European Journal of Mechanics - A/Solids*, Vol. 80, 2020, p. 103874. https://doi.org/10.1016/j.euromechsol.2019.103874, URL https://linkinghub.elsevier.com/retrieve/pii/S0997753819305352.

[33] Goswami, S., Anitescu, C., Chakraborty, S., and Rabczuk, T., "Transfer learning enhanced physics informed neural network for phase-field modeling of fracture," *Theoretical and Applied Fracture Mechanics*, Vol. 106, 2020, p. 102447. https://doi.org/10.1016/j.tafmec.2019.102447, URL https://linkinghub.elsevier.com/retrieve/pii/S016784421930357X.

[34] Lu, L., Pestourie, R., Yao, W., Wang, Z., Verdugo, F., and Johnson, S. G., "Physics-informed neural networks with hard constraints for inverse design," *SIAM Journal on Scientific Computing*, Vol. 43, No. 6, 2021, pp. B1105–B1132.

[35] Kingma, D. P., and Ba, J., "Adam: A method for stochastic optimization," *arXiv preprint arXiv:1412.6980*, 2014.

Downloaded by Abdelrahman Elmaradny on August 29, 2025 | http://arc.aiaa.org | DOI: 10.2514/6.2025-0732